Science Essence Journal Vol. 39 No. 2 (2023) | 63-78

Research Article

Highly Selective and Response NO_2 Gas Sensor Based on Au-Coated ZnO Thin Films

Pitchanunt Chaiyo*

Received: 3 October 2023
Revised: 17 December 2023
Accepted: 18 December 2023

ABSTRACT

This paper investigated the nitrogen dioxide and ammonia gas-sensing properties of Au-coated ZnO thin films obtained by a hybrid method combining atomic layer deposition (ALD) and thermal evaporation techniques. The scanning electron microscopy (SEM) results showed Au nanoparticles, and the thickness of the Au-coated ZnO thin films was approximately 33 nm. X-ray photoelectron spectroscopy (XPS) results confirmed that Au nanoparticles were coated on the surface of the ZnO thin films. The gas sensor based on Au-coated ZnO thin films was tested upon exposure to nitrogen dioxide and ammonia gases with concentrations of 10 ppm to 90 ppm at 250 ^{o}C. Furthermore, the Au-coated ZnO thin films showed an excellent response at a low nitrogen dioxide concentration (10 ppm) with a relative response value of 574%. Moreover, the gas sensor exhibited a high relative and selectivity response to nitrogen dioxide gas.

Keywords: ZnO, Au, gas sensor, NO_2, NH_3

Faculty of Sports and Health Science, Thailand National Sports University Sisaket Campus, Sisaket 33000, Thailand

*Corresponding author, email: Pitchanunt.chaiyo@gmail.com

Introduction

The international air pollution problem has become increasingly urgent because it can cause damage to the human respiratory system. Nitrogen dioxide (NO_2) is the most hazardous and highly toxic gas, a reddish-brown gas or dark brown to yellowish liquid with a strong odor. The combustion of fuels, power plants, automobile exhaust, and chemical factories produces the air pollution. Moreover, nitrogen dioxide can cause photochemical smog, acid rain, and pollution haze [1, 2]. A threshold limit value (TLV) of 5 ppm for short-term NO_2 exposure was set by the U.S. Occupational Safety and Health Administration (OSHA), while the TLV for long-term exposure was set at 100 ppb by the U.S. Environmental Protection Agency (EPA) [3]. Ammonia has corrosive properties and is highly toxic. It can harm eyes, skin, and throat. Particularly, inhaling ammonia gas can harm lungs if inhaled in excess of safe levels. It can cause life-threatening diseases. The Occupational Safety and Health Administration (OSHA) has set an acceptable exposure limit for ammonia to humans at 25 ppm and 35 ppm for 8 hours and 15 minutes, respectively [4]. Therefore, reliable and highly efficient NO_2 and NH_3 gas sensing devices must be developed.

A gas sensing device based on zinc oxide (ZnO) materials has the characteristics of high sensitivity, fast response and recovery times, good selectivity, high electron mobility, stability, operating at room temperature, and low concentration detection [5-9]. They have great advantages for various gas detection, such as acetone, ethanol, benzene, methanol, formaldehyde, ammonia, nitrogen dioxide, carbon monoxide, hydrogen, and hydrogen sulfide gases [10-18]. Zinc oxide is an N-type metal oxide semiconductor (MOS) with a wide band gap of 3.37 eV. Several methods have been used to synthesize zinc oxide materials, for example, hydrothermal, sol-gel, spray pyrolysis, electrochemical anodization, thermal evaporation, precipitation, microwave-assisted, and physical vapor deposition (PVD) [19-26]. Accordingly, a gas sensing device based on zinc oxide with various morphologies, such as nanorods, nanofibers, nanotubes, nanowires, nanoparticles, nanosheets, and thin films, has been advanced for NO_2 gas detection. To improve the gas sensitivity and response in zinc oxide materials, doping is induced either by noble metals such as Ag and Au or transition metals such as Fe, Mn, Cu, and Ni for acting as catalysts [1, 16, 27-30].

Research studies have been reported on the gas sensing device based on zinc oxide materials. Ponnuvelu et al. fabricated hybrid ZnO@Au core–shell nanorods by using a rapid and cost-effective *in situ* chemical synthesis method. The gas sensor based on ZnO@Au core–shell nanorods exhibited good selectivity toward NO_2 and was very stable [31]. Bonyani et al. synthesized Au-decorated ZnO-polyaniline (PANI) composite nanofibers with different amounts of PANI (10, 25, and 50 wt.%) by using electrospinning and coating for NO_2 gas detection. The sensor with 25 wt.%, PANI exhibited the best response to NO_2 gas at 300 °C. Moreover, the optimized sensor showed high selectivity to NO_2 gas [32]. Kim et al. synthesized gold (Au) nanoparticles (NPs)-decorated zinc oxide (ZnO) nanowires (NWs) for nitrogen dioxide (NO_2) gas sensing. The

sensor showed high sensitivity and rapid response to nitrogen dioxide (NO_2) gas at room temperature [33]. Moreover, research studies have reported on the effects of the thickness on thin films for gas sensors. Li et al. fabricated gas sensors based on TiO_2 nano-films with thicknesses of 100 nm, 50 nm, and 30 nm employing a capacitor-like sandwiched Pt/TiO_2/Pt structure for a H_2 gas sensor. The TiO_2 nano-film with a thickness of 30 nm exhibited the highest response to H_2 gas at a concentration of 1000 ppm at 100 °C [34]. Hung et al. synthesized SnS thin films with different thicknesses (30, 50, 80, and 100 nm) for nitrogen dioxide (NO_2) gas sensing. The response of the SnS thin film with a thickness of 30 nm was significantly higher than that of other sensors [35].

In this investigation, the Au-coated ZnO thin films were synthesized by using the hybrid method combining atomic layer deposition (ALD) and thermal evaporation techniques. The advantages of the thermal evaporation method include the ability to adjust the thin film thickness at the nanoscale, as well as its simplicity and low cost [36]. Atomic layer deposition (ALD) method is one of the approaches used to synthesize nanomaterials. The advantages of the ALD method include high-quality films, control over film thickness, high film density, and uniform thickness over large areas. Therefore, thermal evaporation and atomic layer deposition techniques are considered facile methods for preparing pristine ZnO and Au-coated ZnO thin film materials [37]. The dynamic response and recovery cycle of Au-coated ZnO thin films upon exposure to NO_2 and NH_3 gases with concentrations ranging from 10 to 90 ppm at 250 °C was reported. Gas sensing behavior was observed for the Au-coated ZnO thin films toward NO_2 gas with high response and selectivity.

Materials and Methods

Synthesis of Au-coated ZnO thin films

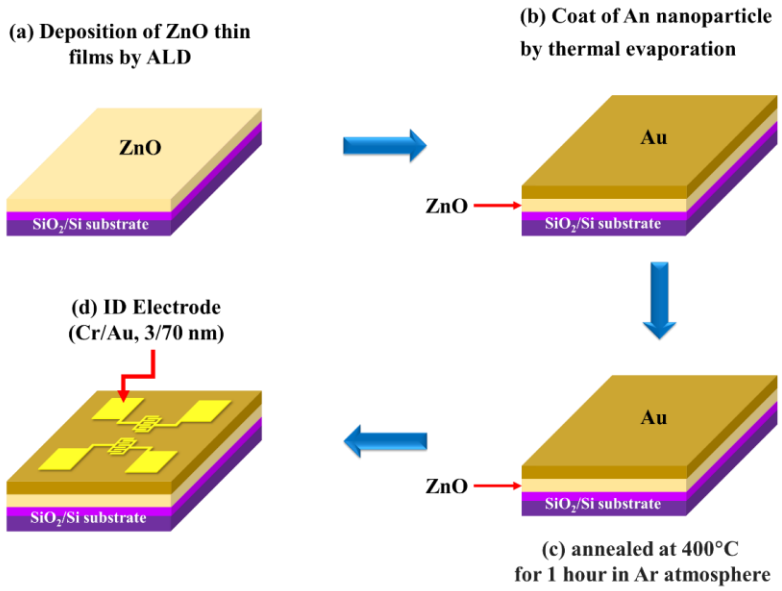

Figure 1 Schematic of synthesized Au-coated ZnO thin films by the two-step method.

First, the ZnO thin films were deposited on SiO_2/Si substrates by the atomic layer deposition method (ALD). The ALD cycles were repeated for 85 cycles at 100 °C by using 10 s of diethyl zinc (DEZ) pulse, 10 s H_2O pulse, and two N_2 purges per cycle. Therefore, the as-synthesized ZnO thin film thickness was 30 nm. Subsequently, a thermal evaporator coated Au nanoparticles onto as-synthesized ZnO thin films with a deposition rate of 0.1 Å/sec. The thickness of the Au nanoparticles on the as-synthesized ZnO thin films was 3 nm. After that, the sample was annealed at 400 °C for 1 h under an Ar atmosphere. Finally, the Au-coated ZnO thin films were successfully synthesized by a hybrid method combining ALD and thermal evaporation techniques, as shown in Figure 1.

Characterization of Au-coated ZnO thin films

A scanning electron microscope (SEM, Hitachi S-4800) was used to investigate the surface morphology of the Au-coated ZnO thin films. X-ray photoelectron spectroscopy (XPS, K-alpha, Thermo Scientific) was used to analyze the valence and composition of the surface elements of pristine ZnO thin films and Au-coated ZnO thin films.

Fabrication and measurement of the Au-coated ZnO thin films gas sensor

The interdigitated electrodes (IDE) (Cr/Au, 3/70 nm) were deposited on the surface of Au-coated ZnO thin films (Figure 1). Subsequently, the response of the sample was measured by using a Keithley-4200 semiconductor parameter analyzer and the responses were examined by exposing them to NO_2 and NH_3 gas with concentrations ranging from 10 to 90 ppm at 250 °C. However, testing gas detectors in response to ammonia gas and nitrogen dioxide gas is conducted at different times. Figure 2 shows the system configuration for a gas sensor.

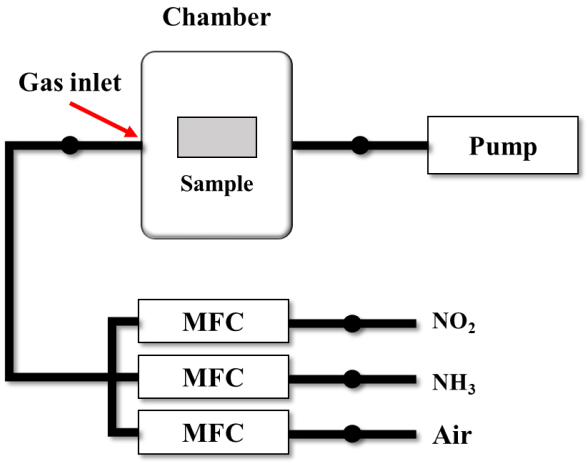

Figure 2 diagram of the gas sensing system.

Results and discussion

Figure 3 shows the surface morphology of the Au-coated ZnO thin films, which were examined by using the SEM technique. The results showed uniformly distributed nanoparticles of gold with a diameter of approximately 10 – 30 nm, as shown in the enlarged SEM images of the Au-coated ZnO thin films (Figure 3(b)). Figure 3(c) shows the cross-section of the Au-coated ZnO thin films. Considering the thickness of the Au-coated ZnO thin films, the results showed that the thin films had a uniform thickness of approximately 33 nm.

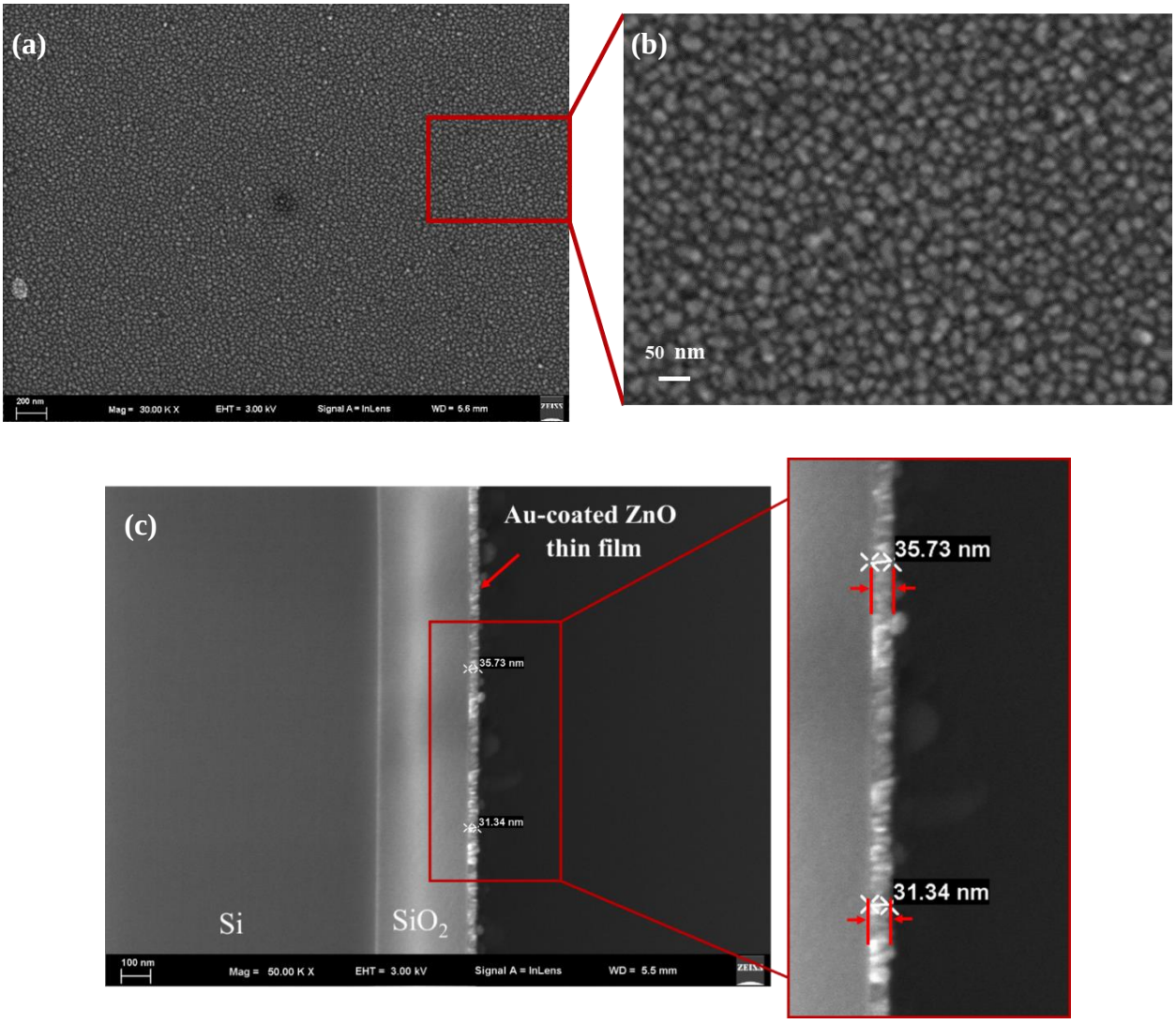

Figure 3 SEM images of (a) Au-coated ZnO thin films, (b) enlarged SEM images of Au-coated ZnO thin films, and (c) the cross-section of Au-coated ZnO thin films.

The components and valence of elements were investigated by using the XPS technique. The survey spectrum of the pristine ZnO thin films showed peaks of Zn, O, and C elements, while the Au-coated ZnO thin films showed the peaks of Zn, O, Au, and C elements, as shown in Figure 4(a). The results clearly showed that the intensity of the ZnO thin films was higher than that of the Au-coated ZnO thin films, especially the peak of Zn 2p. Figure 4(b) shows symmetry peaks of Zn 2p1/2 and Zn 2p3/2, corresponding to binding energies of 1044.2 and 1021.1 eV, respectively. The distance between Zn 2p1/2 and Zn 2p3/2 is 23.1 eV, corresponding to the Zn^{2+} state in both pristine ZnO and Au-coated ZnO thin films [38, 39]. Comparing the spectral Zn 2p1/2 and Zn 2p3/2 peaks of Au-coated ZnO and pristine ZnO thin films, it was found that the Zn 2p1/2 and Zn 2p3/2 peak of Au-coated ZnO thin film was slightly shifted forward by 0.2 eV, which could indicate an increase the electron density due to the coating of Au nanoparticles on the ZnO thin films [38]. The oxygen element peaks of Au-coated ZnO and pristine ZnO thin films are shown in Figure 4(c-d). The results showed that the O 1s peaks of pristine ZnO thin films appear at 530.0, 531.5, and 532.6 eV, which correspond with lattice oxygen (O_L), oxygen vacancy (O_V), and adsorbed oxygen (O_C), respectively. However, the peaks of O_L, O_V, and O_C, Au-coated ZnO appear at 529.8, 531.2, and 532.0 eV, respectively. As a result, the oxygen vacancy (O_V) and adsorbed oxygen (O_C) spectra of Au-coated ZnO thin films increased as compared to that of pristine ZnO thin films, and the lattice oxygen (O_L) spectra of Au-coated ZnO thin films markedly decreased [40]. The percentage of oxygen vacancy (O_V) and adsorbed oxygen (O_C) in Au-coated ZnO thin films increased from 20.17% to 25.93% and from 3.97% to 7.82%, respectively. Therefore, Au-coated ZnO thin films can provide more oxygen vacancy (O_V) and adsorbed oxygen (O_C) than pristine ZnO thin films. For this reason, Au-coated ZnO thin films are useful to improve the gas sensitive properties of the sensor. Because, the Au on the surface of the ZnO thin film facilitates the reaction between the reactive gas and the oxygen atmosphere [41]. The peaks at 88.0 eV and 90.8 eV can be attributed to the Au $4f_{5/2}$ and Zn $3p_{1/2}$, respectively, as shown in Figure 4(e) [42].

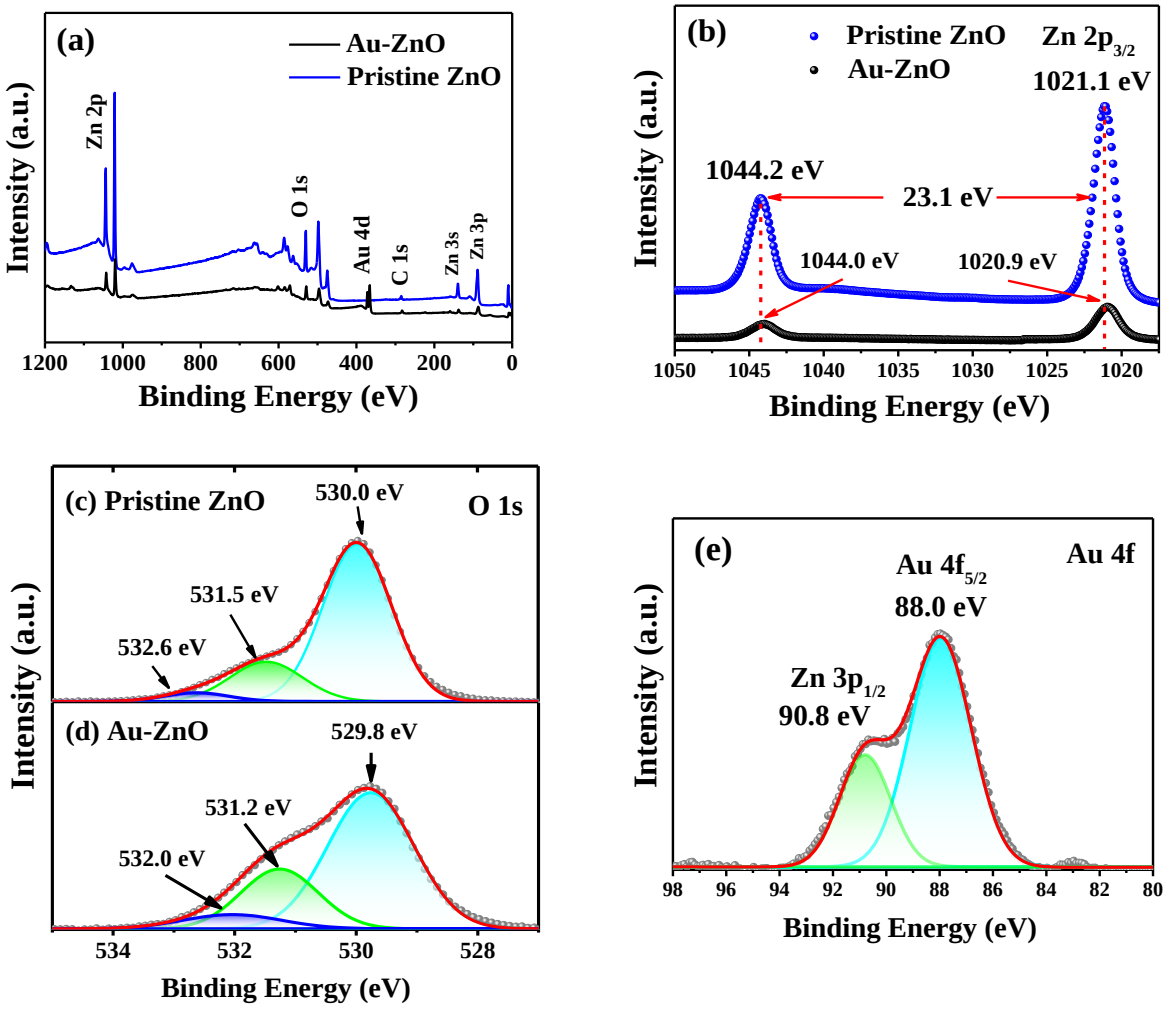

Figure 4 XPS spectra of ZnO and Au-coated ZnO thin films (a) survey spectrum, (b) Zn 2p, (c) O 1s (d) Au-ZnO, and (e) Au 4f-Zn 3p.

The dynamic response curve of the Au-coated ZnO thin films gas sensor is shown in Figure 5. The Au-coated ZnO thin films gas sensor was exposed to NO_2 and NH_3 gases with concentrations ranging from 10 to 90 ppm at 250 °C. The result showed that Au-coated ZnO thin films gas sensor can respond to NO_2 and NH_3 gases at concentrations as low as 10 ppm. High-resolution images of the dynamic response curve of NO_2 and NH_3 gases at a concentration of 20 ppm at 250 °C are shown in Figure 6(a-b). The results showed that the response times (t_{res}) of the Au-coated ZnO thin films gas sensor were 300 and 600 s, corresponding to NO_2 and NH_3 gases, respectively. As a result, the Au-coated ZnO thin films gas sensor reacted significantly faster to NH_3 gas than NO_2 gas. However, the recovery times (t_{rec}) of NH_3 and NO_2 gases of the Au-coated ZnO thin films gas sensor were similar. Figure 6(c–d) shows a high-resolution image of the dynamic response curve of the Au-coated ZnO thin films gas sensor in response to NH_3 and NO_2 gases at concentrations of 80

and 90 ppm at 250 °C. Considering the two cycles in NH_3 gas, the results showed that the Au-coated ZnO thin films gas sensor was able to return to its initial resistance value with a slight difference in resistance in air (R_a), while the resistance value of the Au-coated ZnO thin films gas sensor decreased with increasing concentration of NH_3 gas. In NO_2 gas, the results showed that when the Au-coated ZnO thin films gas sensor was exposed to NO_2 gas, the resistance value increased with increasing concentration of NO_2 gas. As a result, it was shown that the air resistivity of the two loops was 94 and 145 MΩ, corresponding to the gas concentration loops of 80 and 90 ppm. The results showed that as the concentration of NO_2 gas increased, the resistance value of the Au-coated ZnO thin films gas sensor also increased. However, the resistance of the Au-coated ZnO thin films gas sensor could not return to the initial resistance value in air within 3600 s, as shown in Figure 6(d). The initial resistance recovery in NH_3 gas is better than that in NO_2 gas. However, it is possible that the ΔR value of the response to NO_2 gas is approximately 40 times greater than that of NH_3 gas, as shown in Figure 7. Consequently, the resistance while responding to NO_2 gas cannot return to the initial resistance within 3600 s. In contrast, the ΔR value of the response to NH_3 gas is small, allowing the resistance to return to its initial value within 3600 s.

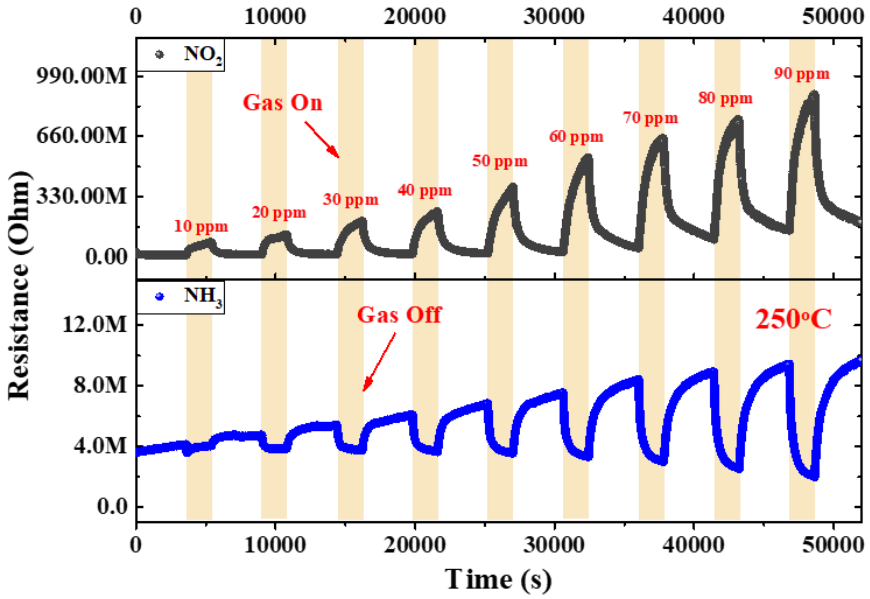

Figure 5 The dynamic response curve of the Au-coated ZnO thin films gas sensor upon exposure to NO_2 and NH_3 gases with concentrations ranging from 10 ppm to 90 ppm at 250 °C.

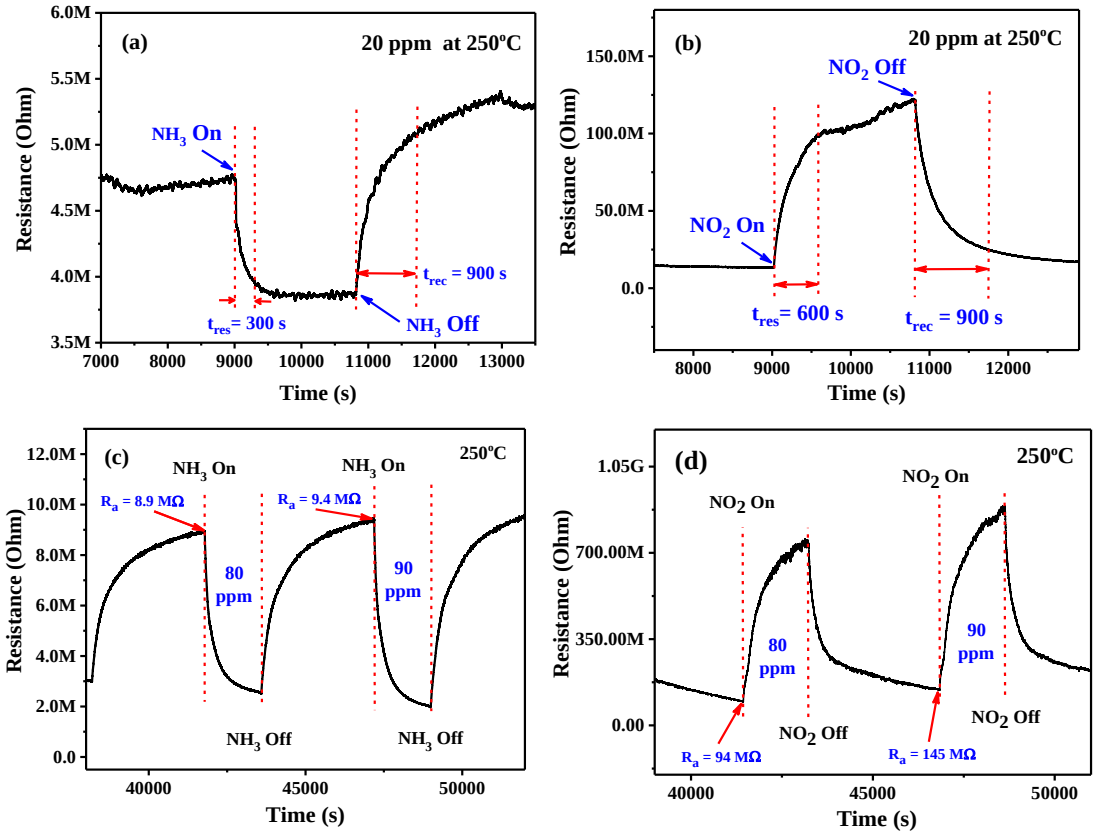

Figure 6 High-resolution images of the dynamic response curve of Au-coated ZnO thin films gas sensor upon exposure to 20 ppm concentration of (a) NH_3 and (b) (NO_2) gases and 80-90 ppm concentrations of (c) NH_3 and (d) NO_2, at 250 ^oC.

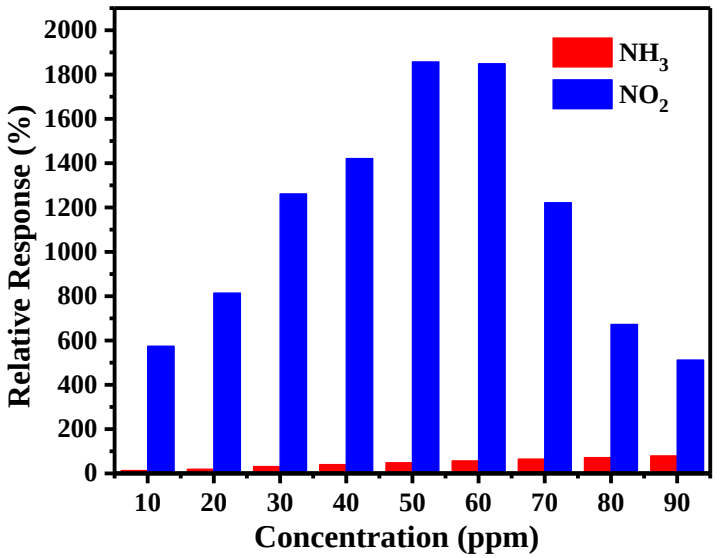

Figure 7 Comparison of the relative response of Au-coated ZnO thin films to NH_3 and NO_2 gases at concentrations ranging from 10 ppm to 90 ppm at 250 ^oC.

A comparison of the relative response of the Au-coated ZnO thin films gas sensor upon exposure to NH_3 and NO_2 gases is presented in Figure 6. The relative response was calculated using equations (1)-(2)

$$\Delta R(\%) = \left(\frac{R_a - R_g}{R_g} \right) \times 100\% \qquad \text{For Reducing gas} \quad (1)$$

$$\Delta R(\%) = \left(\frac{R_g - R_a}{R_a} \right) \times 100\% \qquad \text{For Oxidizing gas} \quad (2)$$

where ΔR is relative response in percent, R_a is resistance in an air atmosphere, and R_g is resistance in a gas atmosphere [43].

To investigate its selectivity, the Au-coated ZnO thin films gas sensor was exposed to NO_2 and NH_3 gases at concentrations ranging from 10 ppm to 90 ppm at 250 ^oC. The relative responses (ΔR) of the Au-coated ZnO thin films gas sensor to 10 - 90 ppm NO_2 gas were 574.17, 814.29, 1261.38, 1420.73, 1857.14, 1848.75, 1221.59, 672.34, and 511.91, respectively. The relative responses of the Au-coated ZnO thin films gas sensor to 10 - 90 ppm NH_3 gas were 13.26, 19.29, 30.94, 39.97, 48.09, 59.29, 64.69, 71.33, and 78.94, respectively. As a result, the results showed that the relative response in NO_2 gas tended to increase in the gas concentration range of 10-50 ppm and decreased in the range of 60-90 ppm. Additionally, the sensor's relative response value in NH_3 gas tended to increase with increasing gas concentration, as shown in Figure 7 (red bar chart). According to the relative response bar chart, the Au-coated ZnO thin films gas sensor responded more to NO_2 than NH_3 gas. Therefore, the gas sensing device based on Au-coated ZnO thin films has a high selective response to NO_2 gas.

Figure 8 shows the mechanism of the Au-coated ZnO thin films gas sensor. Due to the Au-coated ZnO thin films, the gas sensor exhibited n-type semiconductor materials behavior. The sensing mechanism of the gas sensing device can be described by the electron depletion layer theory (EDL). Under an air atmosphere, when the sensor was exposed to air, nearby oxygen molecules were chemisorbed on the surface area of the Au-coated ZnO thin film materials. The chemical reaction of the sensor in an air atmosphere can be explained via the following equations (3)-(6) [43].

$$O_{2(gas)} \longrightarrow O_{2(ads)} \qquad (3)$$

$$O_{2(ads)} + e^- \longrightarrow O^-_{2(ads)} \qquad (T < 100\,^\circ C) \qquad (4)$$

$$O^-_{2(ads)} + e^- \longrightarrow 2O^-_{(ads)} \qquad (100\,^\circ C < T < 300\,^\circ C) \qquad (5)$$

$$O^-_{(ads)} + e^- \longrightarrow O^{2-}_{(ads)} \qquad (T > 300\,^\circ C) \qquad (6)$$

As shown in Figure 8(a), when the Au-coated ZnO thin films gas sensor was exposed to air, the nearly free electrons were captured by the oxygen molecules on the sample's surface area. Therefore, the oxygen molecules become oxygen ions, as shown in equations (4-6), because the surface area of the Au-coated ZnO thin films had a low free electron concentration. As a result, the electron depletion layer of the Au-coated ZnO thin films became wider and increased the resistance value of the sample. When the Au-coated ZnO thin films gas sensor was exposed to NH_3 gas, the resistance of the sensor was lower than the initial resistance value because NH_3 molecules react with oxygen ions, and the captured free electrons were released to the surface area of the sample as shown in equation (7) [44]. However, the Au nanoparticles act as a catalyst for the dissociation of oxygen molecules. The Au nanoparticles on the surface area of the ZnO thin films catalyzed the dissociation of nearly oxygen molecules on its surface area. Therefore, the oxygen molecules were easily separated on the surface area of the Au nanoparticles [44].

$$4NH_{3(ads)} + 3O^{-}_{2(ads)} \longrightarrow N_{2(ads)} + 6H_2O_{(ads)} + 3e^{-} \quad (7)$$

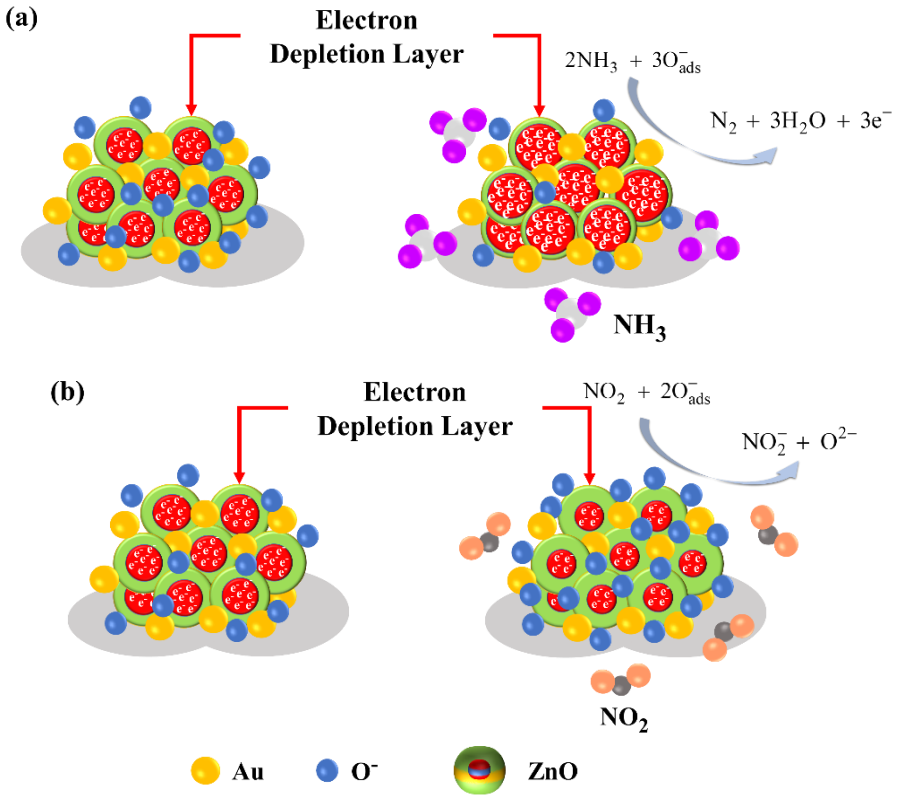

Figure 8 Mechanism of Au-coated ZnO thin films gas sensor upon exposure (a) NH_3 and (b) NO_2 gases.

Figure 8(b) shows the sensing mechanism of the Au-coated ZnO thin films gas sensor exposed to NO_2 gas. This mechanism is divergent from the ammonia gas sensor. In the NO_2 atmosphere, free electrons and oxygen ions are captured by NO_2 molecules and converted to nitrogen dioxide ions, as shown in equations (8-10). As a result, the free electrons concentration is low. Moreover, this reaction causes a lower free electron concentration and a wider electron depletion layer. Therefore, the resistance value of the Au-coated ZnO thin films is greater than the initial resistance value [32, 45].

$$NO_2(g) \longrightarrow NO_2(ads) \tag{8}$$

$$NO_{2(ads)} + e^- \longrightarrow NO_2^- \tag{9}$$

$$NO_2 + 2O^- \longrightarrow NO_2^- + O^{2-} \tag{10}$$

Conclusion

Overall, the Au-coated thin film materials were successfully synthesized by using a hybrid method combining ALD and thermal evaporation techniques. The surface morphology of as-synthesized materials showed a uniform Au nanoparticle on ZnO thin film materials. Moreover, the thickness of the Au-coated thin film materials was approximately 33 nm. The Au-coated ZnO thin films gas sensor responded to NH_3 and NO_2 gases with 10 to 90 ppm concentrations at 250 ^oC. The Au-coated ZnO thin films gas sensing device had a high relative response and high selective response to NO_2 gas. However, the Au-coated ZnO thin film gas sensor exhibited a fast response to ammonia gas, though its relative response was still significantly lower than that of NO_2 gas. Therefore, an Au-coated ZnO thin film gas sensor is suitable for detecting NO_2 gas.

Acknowledgments

The authors are thankful for the Thin Films Materials Research Center at the Korea Research Institute of Chemical Technology for the research facility and financial support. The authors especially thank Dr. Ki-Seok An and Dr. Yeong Min Kwon for help and advice.

References

1. Bonyani M, Zebarjad S, Janghorban K, Kim JY, Kim HW, Kim SS. Au sputter-deposited ZnO nanofibers with enhanced NO_2 gas response. Sens Actuators B Chem. 2022;372:132636.
2. Umar A, Ibrahim AA, Algadi H, Albargi H, Alsairi MA, Wang Y, et al. Supramolecularly assembled isonicotinamide/reduced graphene oxide nanocomposite for room-temperature NO_2 gas sensor. Environ Technol Innov. 2022;25:102066.

3. Li C, Sun YY, Li YN, Zhang XF, D ZP, Huo LH, et al. Low-temperature and high-response NO_2 sensor based on oxygen vacancy-enriched ZnO tubes inherited from waste chestnut mesocarps. Sens Actuators B Chem. 2023;388:133838.
4. Kwak D, Lei Y, Maric R. Ammonia gas sensors: a comprehensive review. Talanta. 2019;204:713-30.
5. Kang SB, Sanger A, Jeong MH, Baik JM, Choi KJ. Heterogeneous stacking of reduced graphene oxide on ZnO nanowires for NO_2 gas sensors with dramatically improved response and high sensitivity. Sens Actuators B Chem. 2023;379:133196.
6. Li B, Liu H, Zeng Q, Dong S, Feng W. Hierarchical porous NiO doped ZnO nanocomposite for formaldehyde gas sensor with high sensitivity, fast response/recovery and good selectivity. Surf Interfaces. 2023;36:102502.
7. Franco MA, Conti PP, Andre RS, Correa DS. A review on chemiresistive ZnO gas sensors. Sens Actuators Rep. 2022;4:100100.
8. Yu X, Chen X, Ding X, Tang K, Zhao X, Liu F. Room temperature ethanol sensor based on ZnO nanoparticles modified by WSe_2 nanosheets. Sens Actuators B Chem. 2023;382:133530.
9. Xuan J, Wang L, Zou Y, Li Y, Zhang H, Lu Q, et al. Room-temperature gas sensor based on in situ grown, etched and W-doped ZnO nanotubes functionalized with Pt nanoparticles for the detection of low-concentration H_2S. J Alloys Compd. 2022;922:166158.
10. Jiang B, Zhou T, Zhang L, Yang J, Han W, Sun Y, et al. Separated detection of ethanol and acetone based on SnO_2-ZnO gas sensor with improved humidity tolerance. Sens Actuators B Chem. 2023;393:134257.
11. Yang M, Gong Y, Shen G, Wang Z, Liu M, Wang Q. Enhanced benzene sensing property of Au-Pd@ZnO and Au-Pt@ZnO core-shell nanoparticles: the function of Pt/Pd decorated Au-ZnO hetero-interface. Mater Lett. 2021;283:128733.
12. Park JY, Kwak Y, Lim HR, Park SW, Lim MS, Cho HB, et al. Tuning the sensing responses towards room-temperature hypersensitive methanol gas sensor using exfoliated graphene-enhanced ZnO quantum dot nanostructures. J Hazard Mater. 2022;438:129412.
13. Huang J, Liang H, Ye J, Jiang D, Sun Y, Li X, et al. Ultrasensitive formaldehyde gas sensor based on Au-loaded ZnO nanorod arrays at low temperature. Sens Actuators B Chem. 2021;346:130568.
14. Kanaparthi S, Singh SG. Highly sensitive and ultra-fast responsive ammonia gas sensor based on 2D ZnO nanoflakes. Mater Sci Energy Technol. 2020;3:91-6.
15. Tseng SF, Chen PS, Hsu SH, Hsiao WT, Peng WJ. Investigation of fiber laser-induced porous graphene electrodes in controlled atmospheres for ZnO nanorod-based NO_2 gas sensors. Appl Surf Sci. 2023;620:156847.

16. Wang Y, Cui Y, Meng X, Zhang Z, Cao J. A gas sensor based on Ag-modified ZnO flower-like microspheres: temperature-modulated dual selectivity to CO and CH_4. Surf Interfaces. 2021;24:101110.
17. Kim JH, Mirzaei A, Kim HW, Wu P, Kim SS. Design of supersensitive and selective ZnO-nanofiber-based sensors for H_2 gas sensing by electron-beam irradiation. Sens Actuators B Chem. 2019;293:210-223.
18. Hanh To DT, Park JY, Yang B, Myung NV, Choa YH. Nanocrystalline ZnO quantum dot-based chemiresistive gas sensors: improving sensing performance towards NO_2 and H_2S by optimizing operating temperature. Sens Actuators Rep. 2023;6:100166.
19. Vaddi DR, Vinukonda K, Patnala RK, Kanithi Y, Gurugubelli TR, Bae J, et al. Effect of yttrium doping on the crystal structure, optical, and photocatalytic properties of hydrothermally synthesized ZnO nanorods. Mater Sci Eng B. 2023;296:116664.
20. Liu Z, Hu R, Yu J, Wang R, Cheng J, Huo Mm, et al. Fabrication of ZnO interface layer from a novel aqueous sol-gel precursor solution for organic solar cells. Synth Met. 2021;274:116737.
21. Cuadra JG, Estrada AC, Oliveira C, Abderrahim LA, Porcar S, Fraga D, et al. Functional properties of transparent ZnO thin films synthetized by using spray pyrolysis for environmental and biomedical applications. Ceram Int. 2023;49: 32779-88.
22. Tello A, Boulett A, Sanchez J, Pizarro GC, Soto C, Perez OEL, et al. An unexplored strategy for synthesis of ZnO nanowire films by electrochemical anodization using an organic-based electrolyte. Morphological and optical properties characterization. Chem Phys Lett. 2021;778:138825.
23. Abdallah B, Kakhia M, Zetoun W, Alkafri N. PbS doped ZnO nanowires films synthesis by thermal evaporation method: morphological, structural and optical properties. Microelectron J. 2021;111:105045.
24. Rezaei A, Katoueizadeh E, Zebarjad SM. Investigation of the parameters affecting the morphology of zinc oxide (ZnO) nanoparticles synthesized by precipitation method. Microelectron J. 2022;26:101239.
25. Perez-Cuapio R, Alvarado JA, Juarez H, Sue HJ. Sun irradiated high efficient photocatalyst ZnO nanoparticles obtained by assisted microwave irradiation. Mater Sci Eng B. 2023;289:116263.
26. Saravanavel G, Honnali SK, Lourdes KS, John S, Gunasekhar KR. Study on the thermoelectric properties of Al-ZnO thin-film stack fabricated by physical vapour deposition process for temperature sensing. Sens Actuators A Phys. 2021;332:113097.
27. Seddik B, Salima B, Houda G. Fe doped ZnO nanostructures prepared via sol-gel dip-coating technique for iso-butane (i-C4H10) sensing. Mater Today Commun. 2021;29:102805.

28. Ramesh A, Gavaskar DS, Nagaraju P, Duvvuri S, Vanjari SRK, Subrahmanyam C. Mn-doped ZnO microspheres prepared by solution combustion synthesis for room temperature NH3 sensing. Appl Surf Sci Adv. 2022;12:100349.
29. Kamble VS, Zemase RK, Gupta RH, Aghav BD, Shaikh SA, Pawara JM, et al. Improved toxic NO2 gas sensing response of Cu-doped ZnO thin-film sensors derived by simple co-precipitation route. Opt Mater. 2022;131:112706.
30. Lokhande SD, Awale MB, Umadevi G, Mote VD. Effect of Ni doping on structural, optical and gas sensing properties of ZnO films for the development of acetone sensor devices. Mater Chem Phys. 2023;301:127667.
31. Ponnuvelu DV, Pullithadathil B, Prasad AK, Dhara S, Ashok A, Mohamed K, et al. Rapid synthesis and characterization of hybrid ZnO@Au core–shell nanorods for high performance, low temperature NO_2 gas sensor applications. Appl Surf Sci. 2015;355:726-35.
32. Bonyani M, Zebarjad SM, Janghorban K, Kim JY, Kim HW, Kim SS. Au-Decorated Polyaniline-ZnO Electrospun Composite Nanofiber Gas Sensors with Enhanced Response to NO_2 Gas. Chemosensors. 2022;10(10):338.
33. Kim DW, Park KH, Lee SH, Fabrega C, Prades D, Jang JW. Plasmon expedited response time and enhanced response in gold nanoparticles-decorated zinc oxide nanowire-based nitrogen dioxide gas sensor at room temperature. J Colloid Interface Sci. 2021;582:658-68.
34. Li Z, Haidry AA, Plecenik T, Vidis M, Grancic B, Roch T, et al. Influence of nanoscale TiO_2 film thickness on gas sensing properties of capacitor-like Pt/TiO_2/Pt sensing structure. Appl Surf Sci. 2020;499:143909.
35. Hung NM, Nguyen C, Arepalli VK, Kim J, Chinh ND, Nguyen TD, et al. Defect-induced gas-sensing properties of a flexible SnS sensor under UV illumination at room temperature. Sensors. 2020;20(19):5701.
36. Ozkartal A, Noori DT. Effects of thermal annealing on the characterization of p-NiO/n-GaAs heterojunctions produced by thermal evaporation. J Mater Sci Mater Electron. 2021;32:13462–71.
37. Oviroh PO, Akbarzadeh R, Pan D, Coetzee RAM, Jen TC. New development of atomic layer deposition: processes, methods and applications. Sci Technol Adv Mater. 2019;20(1):465-96.
38. Tang JF, Fang CC, Hsu CL. Enhanced organic gas sensor based on Cerium- and Au-doped ZnO nanowires via low temperature one-pot synthesis. Appl Surf Sci. 2023;613:156094.
39. Li X, Zhu G, Dou J, Yang J, Ge Y, Liu J. Electrospun Au nanoparticle-containing ZnO nanofiber for non-enzyme H_2O_2 sensor. Ionics. 2019;25:5527-36.

40. Zhao C, Xu S, Wei J, Xie S, Wei J, Han J, et al. Enhanced response for foodborne pathogens detection by Au nanoparticles decorated ZnO nanosheets gas sensor. Biosensors. 2022;12(10):803.
41. Aswal DK, Gupta SK. Science and technology of chemiresistor gas sensors. New York: Nova Science Publishers; 2007.
42. Bai L, Mei J. Low amount of Au nanoparticles deposited ZnO nanorods heterojunction photocatalysts for efficient degradation of p-nitrophenol. J Sol-Gel Sci Technol. 2020;94:468-76.
43. Krishna KG, Parne S, Pothukanuri N, Kathirvelu V, Gandi S, Joshi D. Nanostructured metal oxide semiconductor-based gas sensors: a comprehensive review. Sens Actuator Phys. 2022;341:113578.
44. Shingange K, Tshabalala ZP, Ntwaeaborwa OM, Motaung DE, Mhlongo GH. Highly selective NH_3 gas sensor based on Au loaded ZnO nanostructures prepared using microwave-assisted method. J Colloid Interface Sci. 2016;479:127-38.
45. Sun M, Wang M, Ge C, Huang J, Li Y, Yan P, et al. Au-doped ZnO@ZIF-7 core-shell nanorod arrays for highly sensitive and selective NO_2 detection. Sens Actuators B Chem. 2023;384:133632.